

Agricultural Drought Detection with MODIS Based Vegetation Health Indices in Southeast Germany

Simon Kloos ^{1,*}, Ye Yuan ¹, Mariapina Castelli ² and Annette Menzel ^{1,3,*}

¹ TUM School of Life Sciences, Ecoclimatology, Technical University of Munich; Freising, 85354, Germany; simon.kloos@tum.de; yuan@wzw.tum.de

² Institute for Earth Observation, Eurac Research; Bolzano/Bozen, 39100, Italy; mariapina.castelli@eurac.edu

³ Institute for Advanced Study, Technical University of Munich; Garching, 85748, Germany; annette.menzel@tum.de

* Correspondence: simon.kloos@tum.de

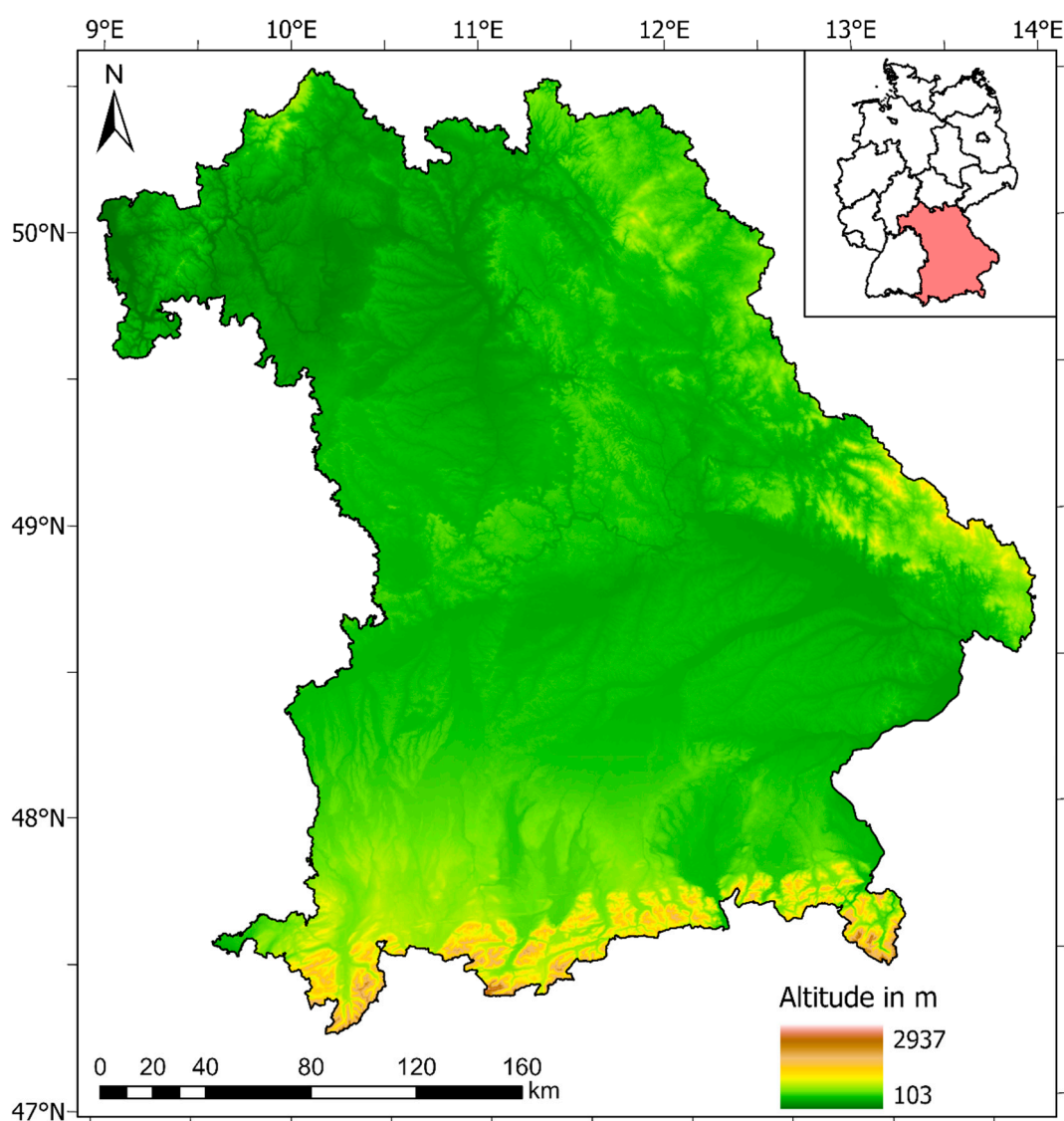


Figure S1. Map of altitude distribution in Bavaria. High-altitude areas are located mainly on the edge of the Alps in the south of the area and the eastern border region. The lowest-lying part of Bavaria is in the northwest (Data: EU-DEM v1.1).

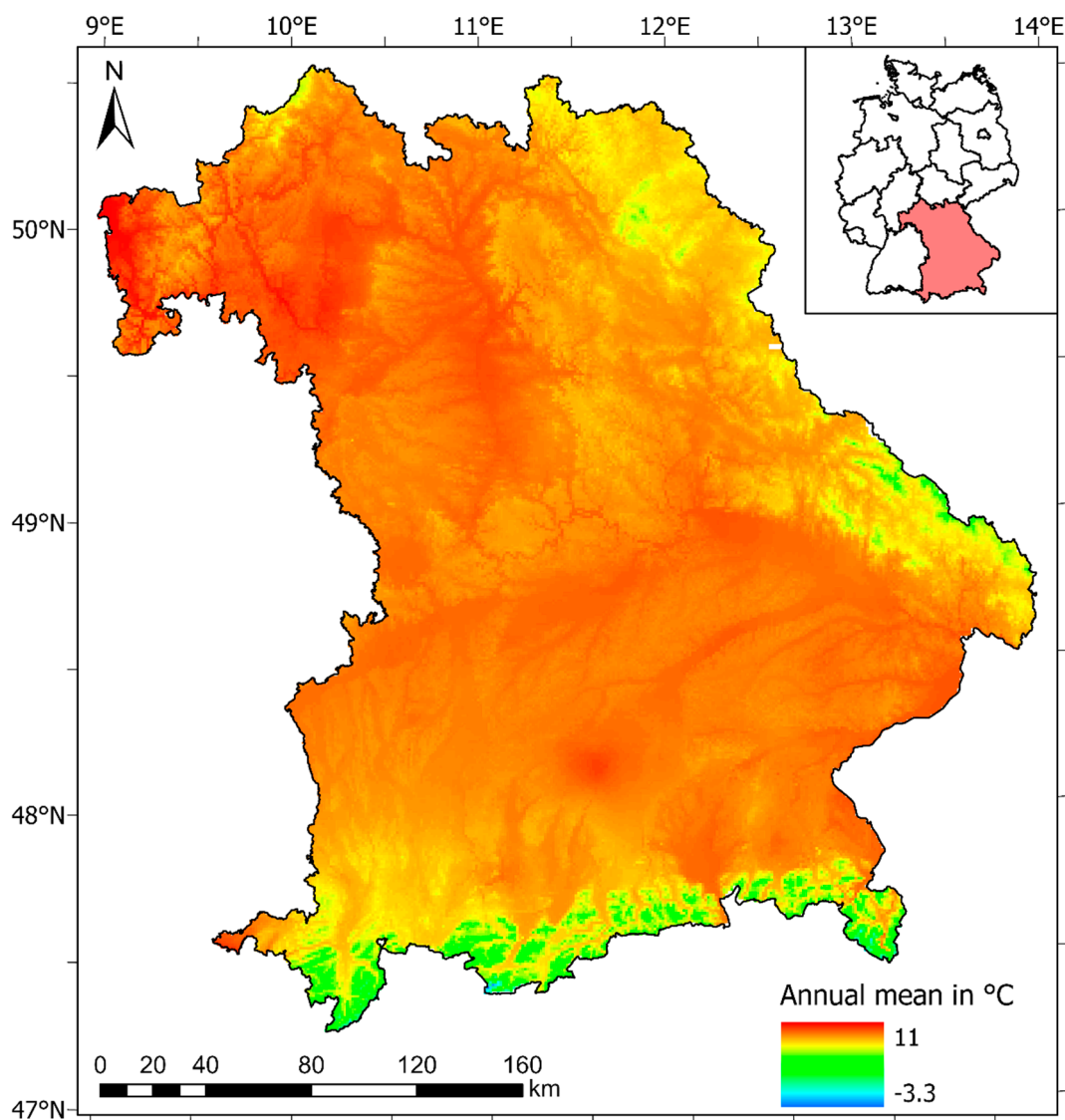


Figure S2. Overview map of mean annual air temperature (2 m) for Bavaria from 1991-2020. Here, the dependence of temperature on altitude (Figure S1) becomes clear: The lowest annual temperatures are found in the Alpine region and eastern Bavaria, while the highest temperatures occur in northwestern Bavaria (Data: German Meteorological Service).

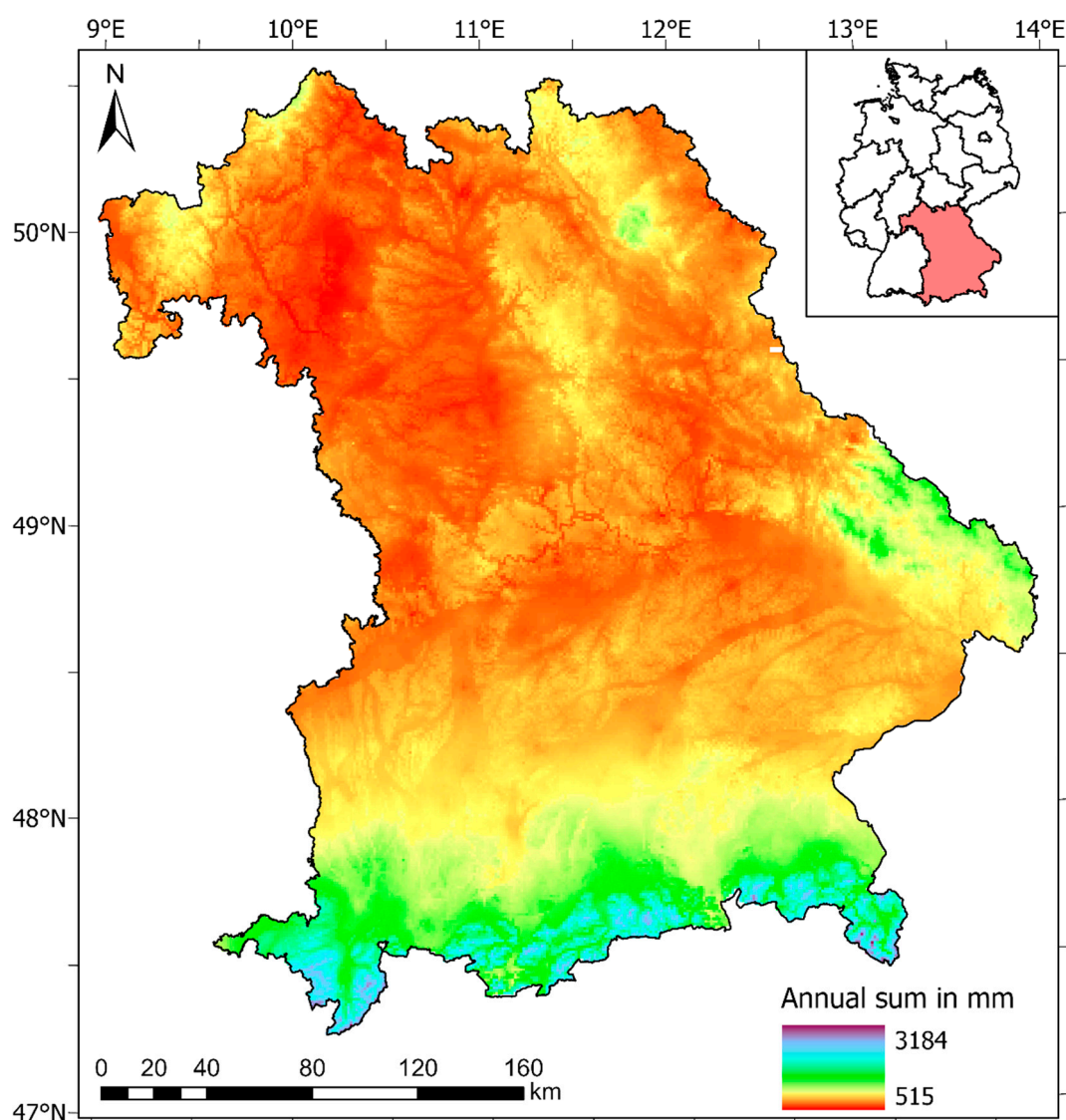


Figure S3. Overview map of mean annual precipitation sum in Bavaria from 1991-2020. Here, too, the dependence of annual precipitation on altitude (Figure S1) is obvious: Significantly more precipitation falls in the south and east of Bavaria, than in the rest of the study area (Data: German Meteorological Service).

Table S1. Simplified land cover classification according to CLC 2018 classification applied in Figure 2.

Simplified land cover classes	Land cover classes: CLC 2018
Urban Areas	Continuous urban fabric
	Discontinuous urban fabric
	Industrial or commercial units
	Road and rail networks and associated land
	Port areas
	Airports
	Mineral extraction sites
	Dump-sites
	Construction sites

	Green urban areas
	Sport and leisure facilities
Agriculture	Non-irrigated arable land
	Permanently irrigated land
	Rice fields
	Vineyards
	Fruit trees and berry plantations
	Olive groves
	Pastures
	Annual crops associated with permanent crops
	Complex cultivation patterns
	Land principally occupied by agriculture with significant areas of natural vegetation
	Agro-forestry areas
Forest	Broad-leaved forest
	Coniferous forest
	Mixed forest
Grassland	Natural grasslands
	Moors and heathland
	Sclerophyllous vegetation
	Transitional woodland-shrub
Bare	Beaches dunes sands
	Bare rocks
	Sparsely vegetated areas
	Burnt areas
Snow and Glacier	Glaciers and perpetual snow
Wetlands	Inland marshes
	Peat bogs
	Salt marshes
	Salines
	Intertidal flats
Water Bodies	Water-courses
	Water bodies
	Coastal lagoons
	Estuaries
	Sea and ocean

Table S2. Classification of the MCD12Q1 International Geosphere-Biosphere Programme (IGBP) classes into the vegetation mask and the non-vegetation mask.

Mask	Name	Description
Vegetation	Evergreen Needleleaf Forests	Dominated by evergreen conifer trees (canopy >2 m). Tree cover >60%.
	Evergreen Broadleaf Forests	Dominated by evergreen broadleaf and palmate trees (canopy >2 m). Tree cover >60%.

	Deciduous Needleleaf Forests	Dominated by deciduous needleleaf (larch) trees (canopy >2 m). Tree cover >60%.
	Deciduous Broadleaf Forests	Dominated by deciduous broadleaf trees (canopy >2 m). Tree cover >60%.
	Mixed Forests	Dominated by neither deciduous nor evergreen (40-60% of each) tree type (canopy >2 m). Tree cover >60%.
	Closed Shrublands	Dominated by woody perennials (1-2 m height) >60% cover.
	Open Shrublands	Dominated by woody perennials (1-2 m height) 10-60% cover.
	Woody Savannas	Tree cover 30-60% (canopy >2 m).
	Savannas	Tree cover 10-30% (canopy >2 m).
	Grasslands	Dominated by herbaceous annuals (<2 m).
	Croplands	At least 60% of area is cultivated cropland.
	Cropland/Natural Vegetation Mosaics	Mosaics of small-scale cultivation 40-60% with natural tree, shrub, or herbaceous vegetation.
Non-Vegetation	Permanent Wetlands	Permanently inundated lands with 30-60% water cover and >10% vegetated cover.
	Urban and Built-up Lands	At least 30% impervious surface area including building materials, asphalt, and vehicles.
	Permanent Snow and Ice	At least 60% of area is covered by snow and ice for at least 10 months of the year.
	Barren	At least 60% of area is non-vegetated barren (sand, rock, soil) areas with less than 10% vegetation.
	Water Bodies	At least 60% of area is covered by permanent water bodies.

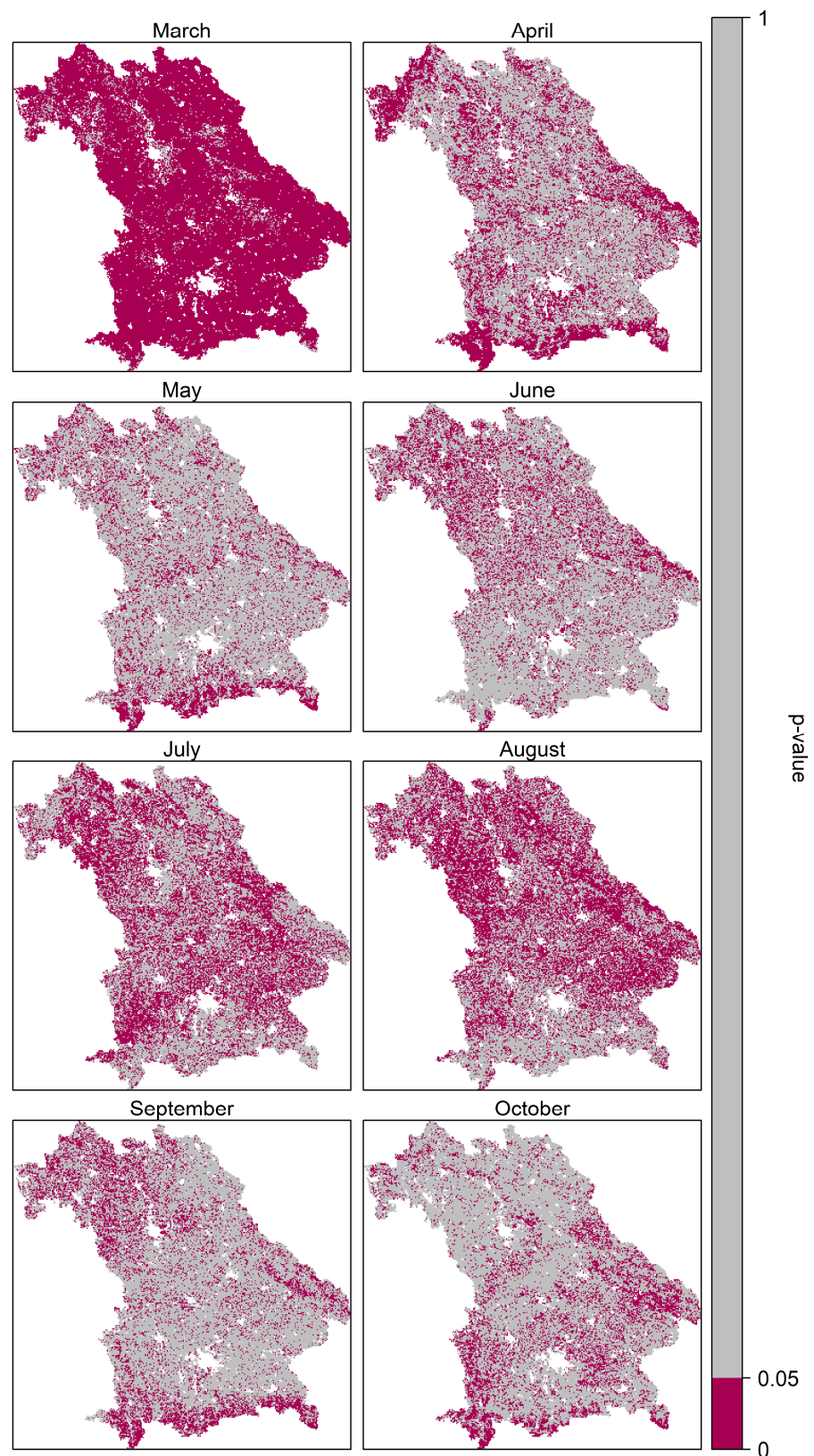
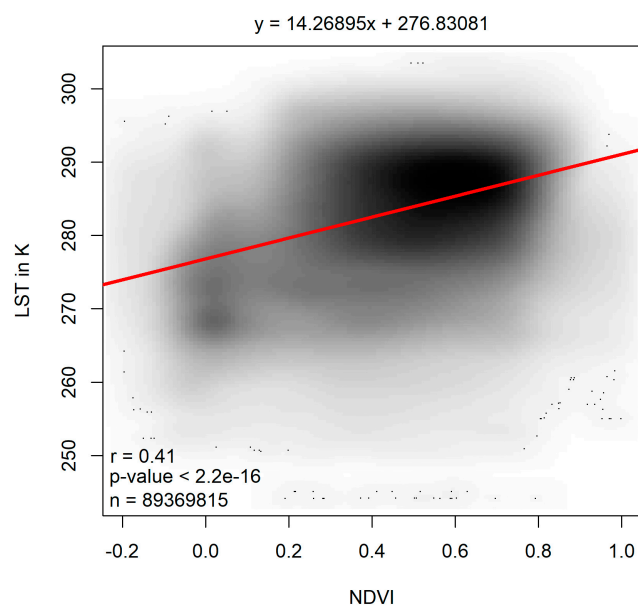


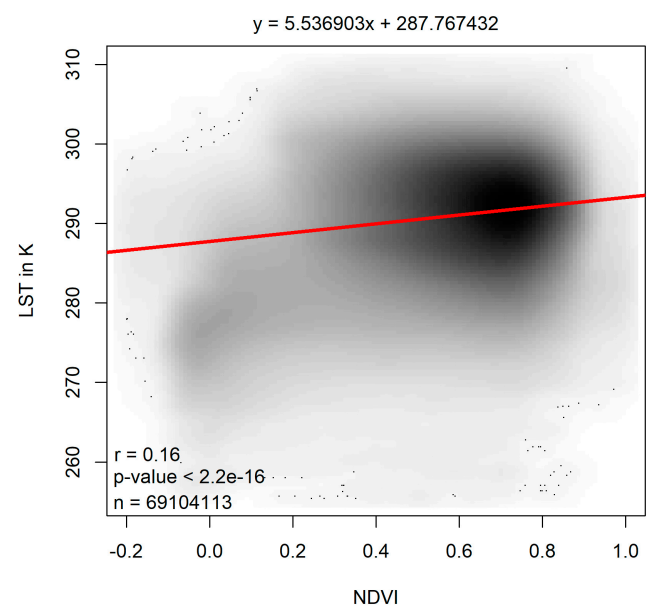
Figure S4. P-values of the pixel-based monthly correlation coefficients (Bravais-Pearson) between NDVI and LST in Bavaria from 2001 to 2020 during the vegetation period (March to October; Figure 3). The purple-colored pixels represent all areas in the respective month which have a p-value < 0.05 and thus a statistically significant correlation.

Table S3. Pixel-based monthly correlation coefficients (Bravais-Pearson) between NDVI and LST in Bavaria from 2001 to 2020 during the vegetation period (March to October; Figure 3). The gray tone of the cell increases with the percentage amount (maximum: 100%). The range between >-0.1 and 0.1 (no correlation) is marked separately.

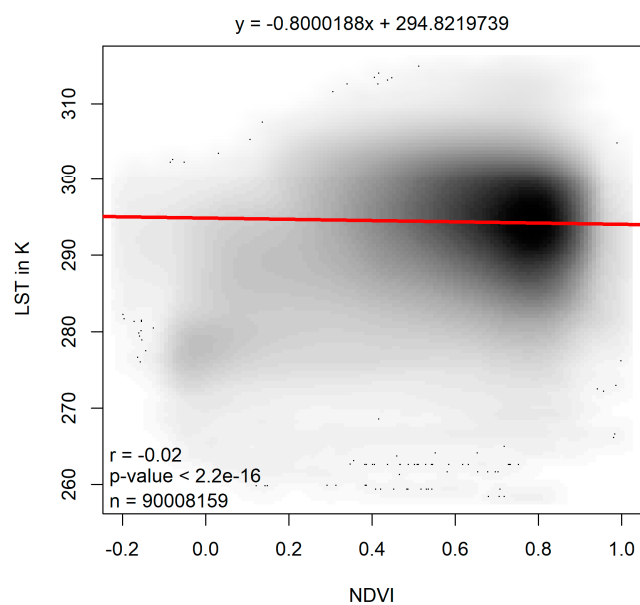
r	March	April	May	June	July	August	September	October
-1.0 to -0.7	0.00%	0.00%	0.00%	0.00%	0.01%	0.03%	0.00%	0.00%
>-0.7 to 0.5	0.00%	0.00%	0.01%	0.14%	2.46%	5.80%	0.04%	0.00%
>0.5 to -0.3	0.02%	0.49%	1.44%	6.13%	23.14%	24.19%	3.43%	0.24%
>0.3 to -0.1	0.13%	7.51%	16.70%	28.04%	36.65%	28.80%	20.58%	5.70%
>-0.1 to 0.1	1.36%	26.99%	39.63%	38.23%	25.94%	23.34%	36.72%	31.14%
>0.1 to 0.3	10.24%	35.76%	33.20%	21.22%	10.62%	14.90%	31.45%	45.93%
>0.3 to 0.5	40.67%	23.14%	8.20%	5.86%	1.17%	2.80%	7.49%	15.81%
>0.5 to 0.7	41.85%	5.47%	0.69%	0.37%	0.02%	0.13%	0.29%	1.14%
>0.7 to 1.0	5.73%	0.63%	0.12%	0.01%	0.00%	0.00%	0.01%	0.02%



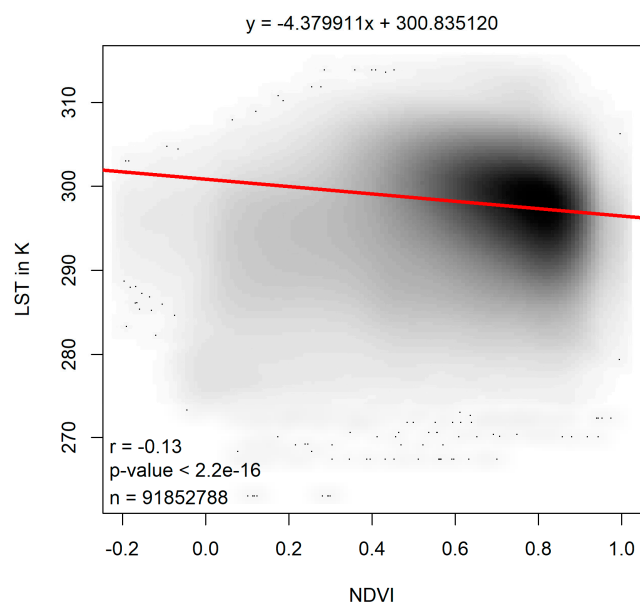
(a)



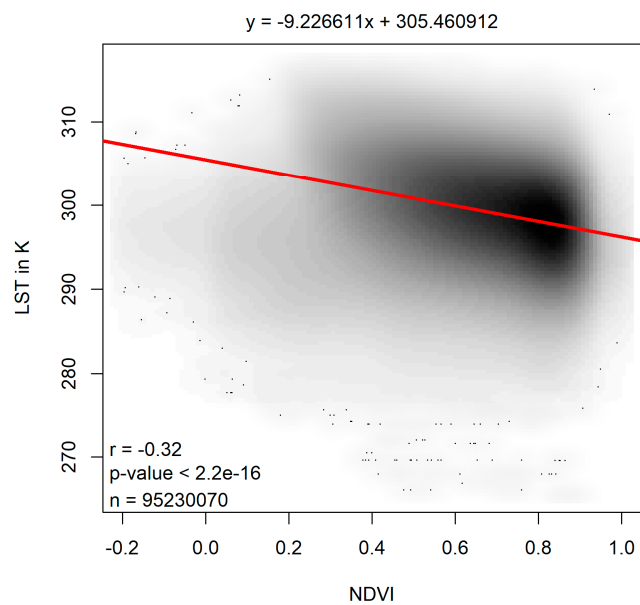
(b)



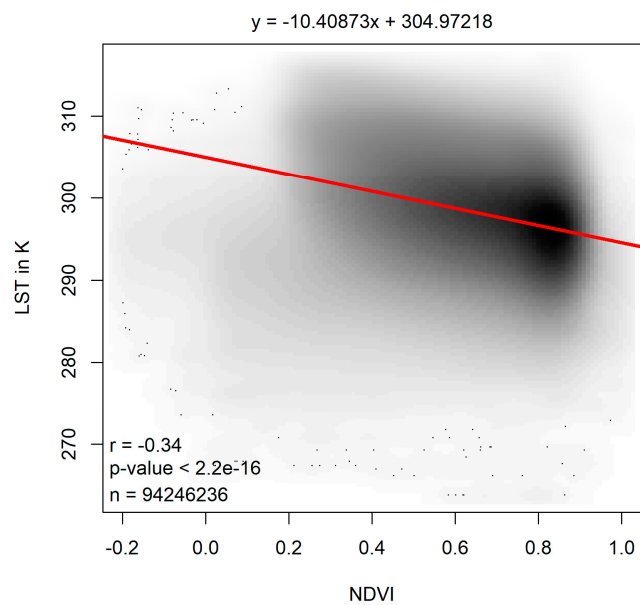
(c)



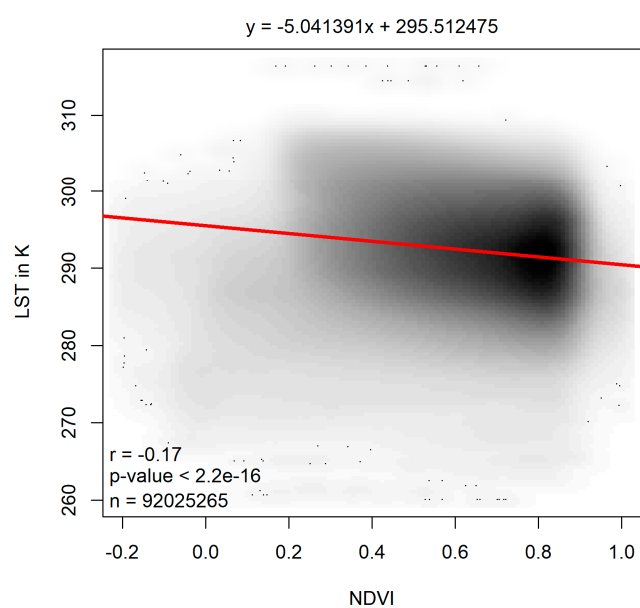
(d)



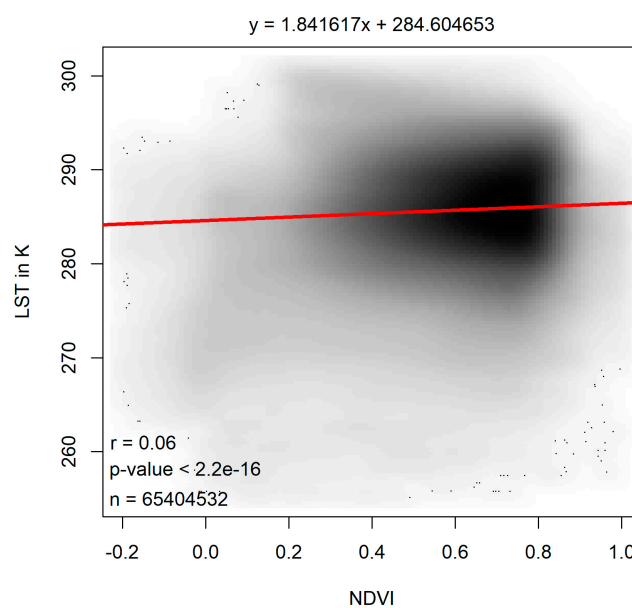
(e)



(f)



(g)



(h)

Figure S5. Pixel-based scatterplot between 8-day NDVI and LST in Bavaria from 2001 to 2020 in March (a), April (b), May (c), June (d), July (e), August (f), September (g), October (h; Figure 3). The red line represents the regression line associated to the regression equation (above the plot). r represents the correlation coefficient (according to Bravais-Pearson), the corresponding p-value and the number of value pairs are given.

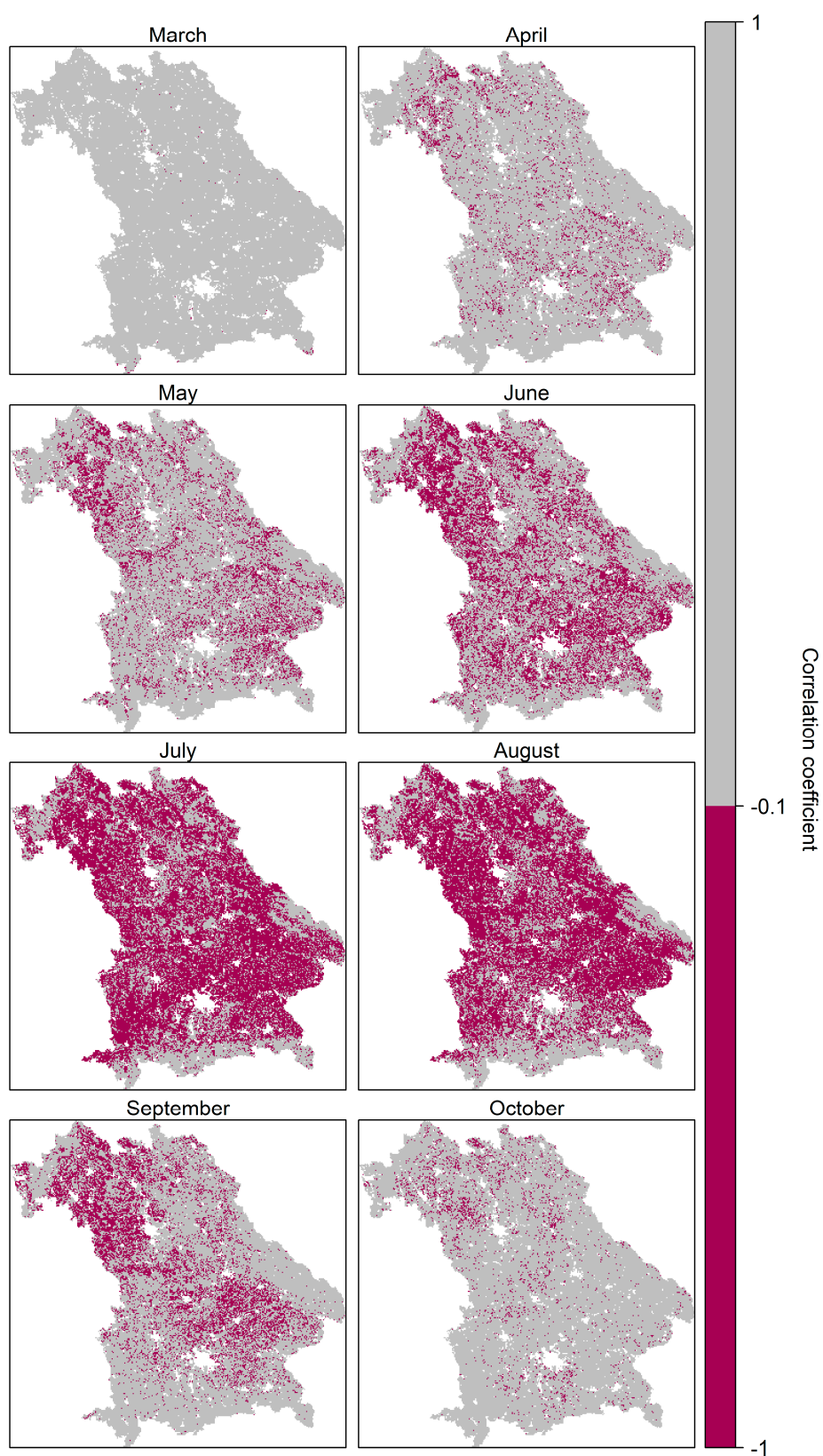


Figure S6. Pixel-based monthly correlation coefficients (Bravais-Pearson) between NDVI and LST in Bavaria from 2001 to 2020 during the vegetation period (March to October). The purple-colored pixels represent all areas in the respective month which are classified by a correlation coefficient ≤ -0.1 . These areas have thus been included in the application and validation of the calculated drought indices.

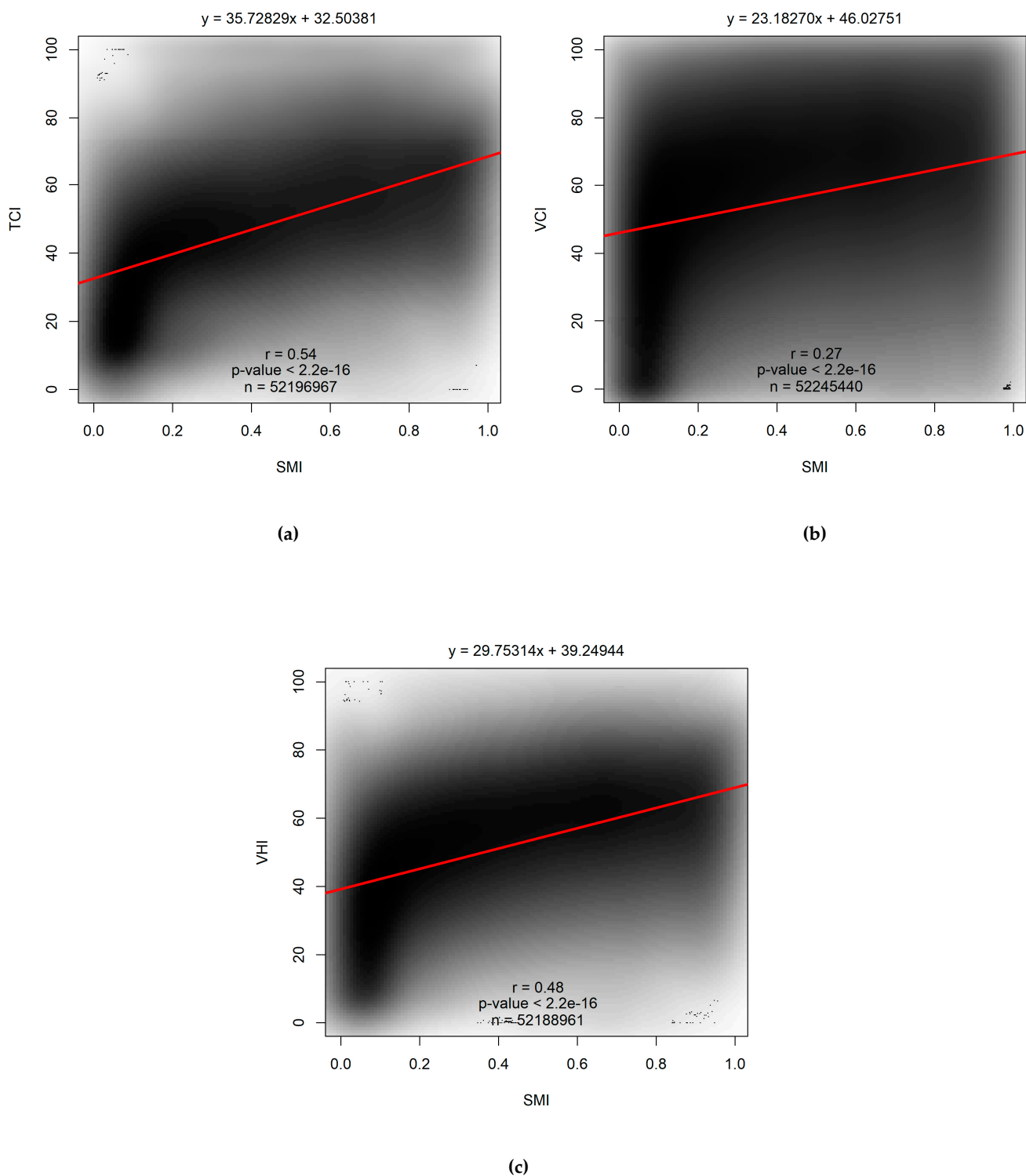


Figure S7. Pixel-based scatterplot between SMI and TCI (a), VCI (b) and VHI (c) in Bavaria from 2001 to 2020 (March to October). The red line represents the regression line associated to the regression equation (above the plot). r represents the correlation coefficient (according to Bravais-Pearson), the corresponding p-value and the number of value pairs are given.

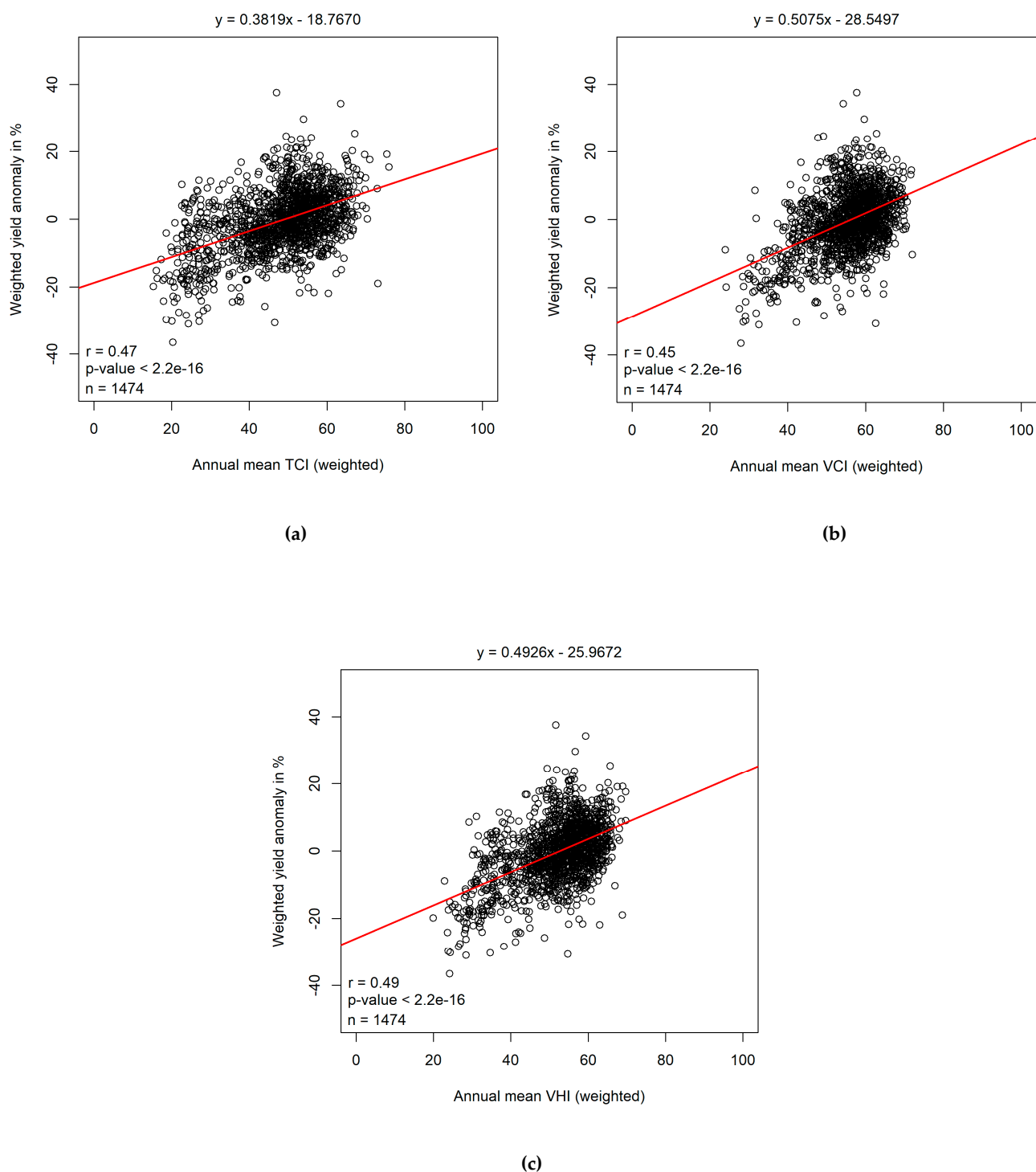


Figure S8. Scatterplot between weighted yield anomaly and weighted annual mean TCI (a), VCI (b) and VHI (c) in Bavaria from 2001 to 2019 (county level). The red line represents the regression line associated to the regression equation (above the plot). r represents the correlation coefficient (according to Bravais-Pearson), the corresponding p-value and the number of value pairs are given.

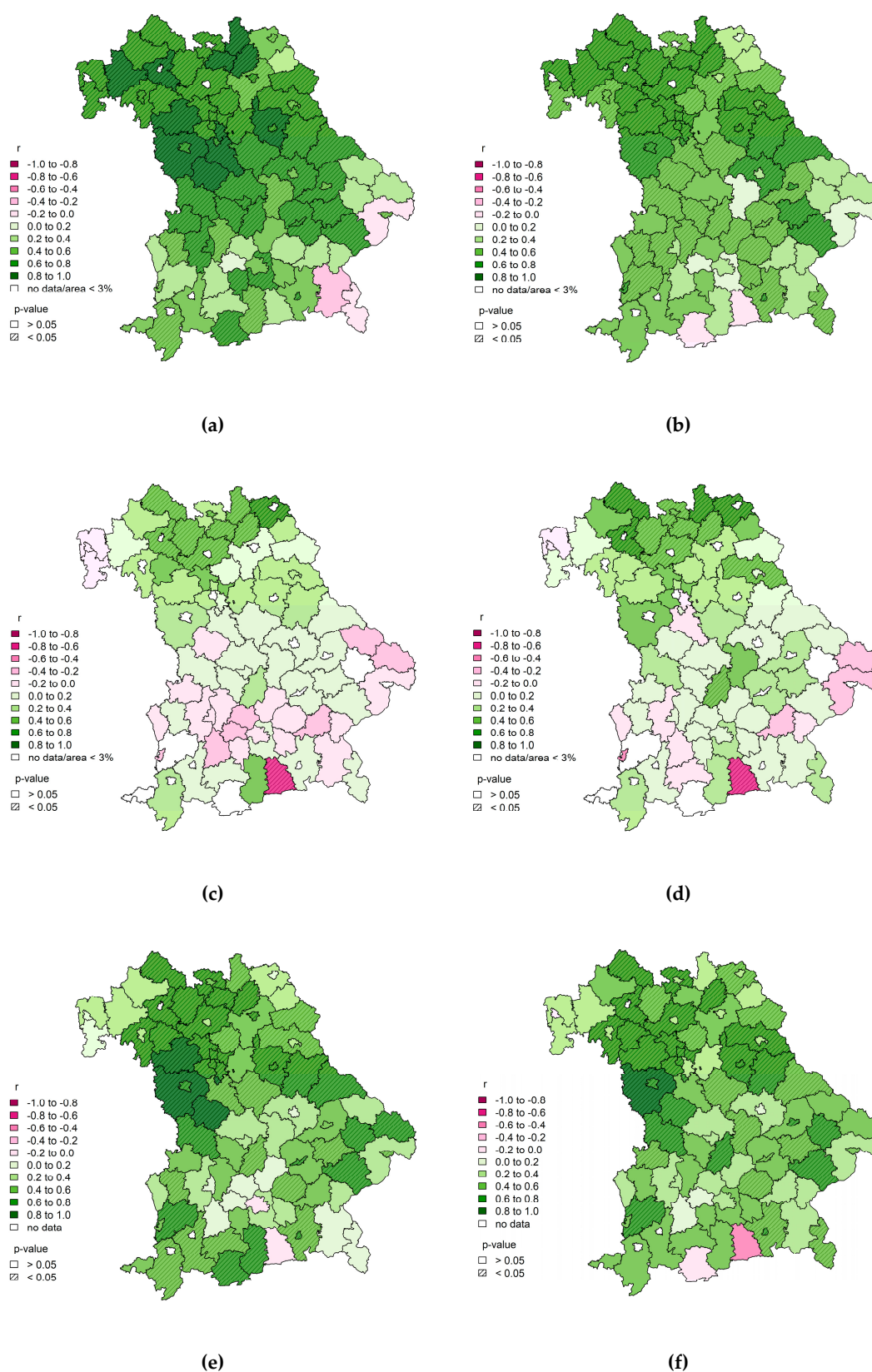


Figure S9. Bravais-Pearson correlation coefficients between the relative annual silage corn yield anomalies and the annual mean TCI (a) or VCI (b), the relative annual winter wheat yield anomalies and the annual mean TCI (c) or VCI (d), and the annual relatively weighted crop yield anomalies and the annual weighted TCI (e) or VCI (f) differentiated by county.

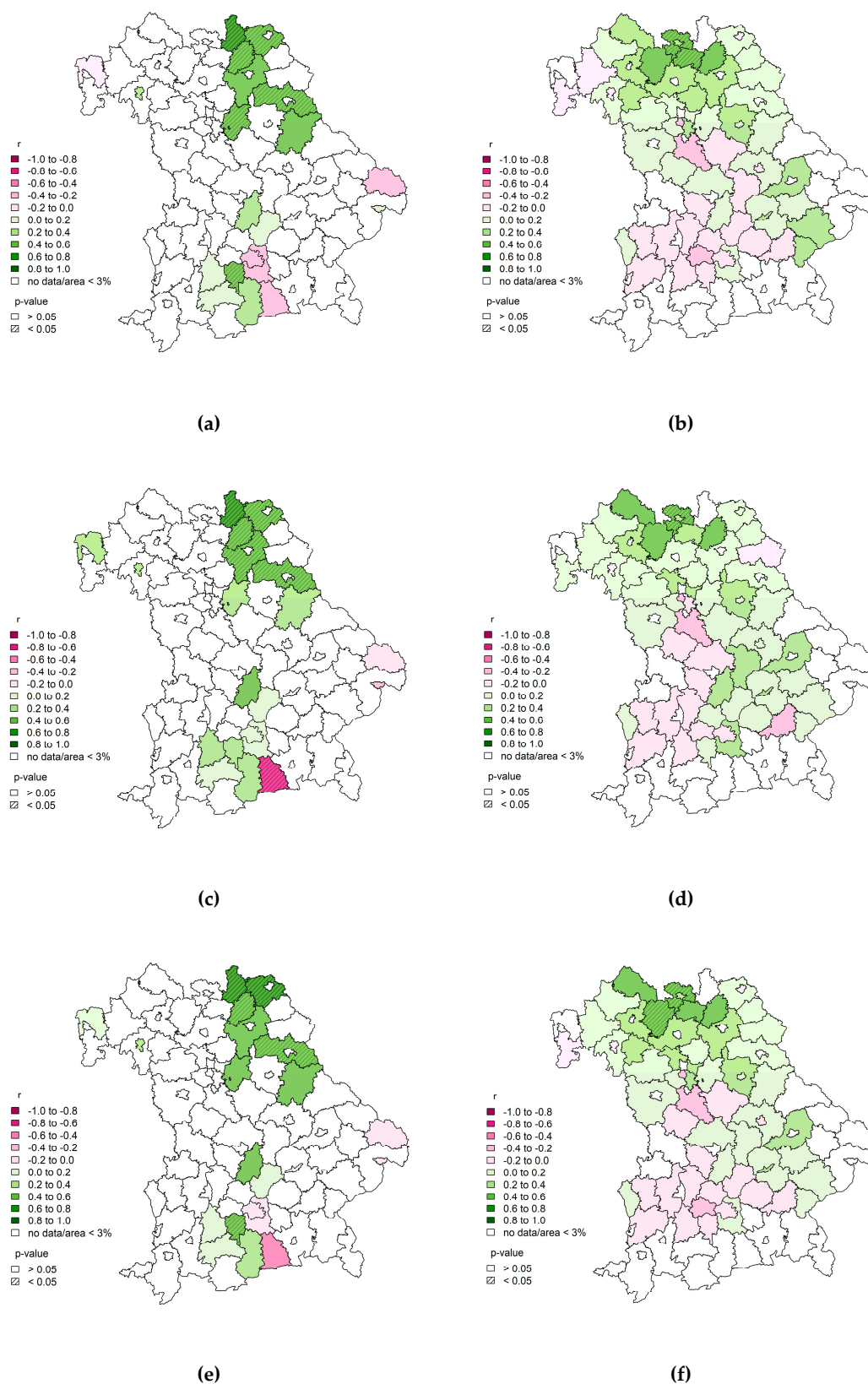


Figure S10. Bravais-Pearson correlation coefficients between the relative annual oat yield anomalies and the annual mean TCI (a)/VCI (c)/VHI (e) and the relative annual winter rapeseed yield anomalies and the annual mean TCI (b)/VCI (d)/VHI (f) differentiated by county.

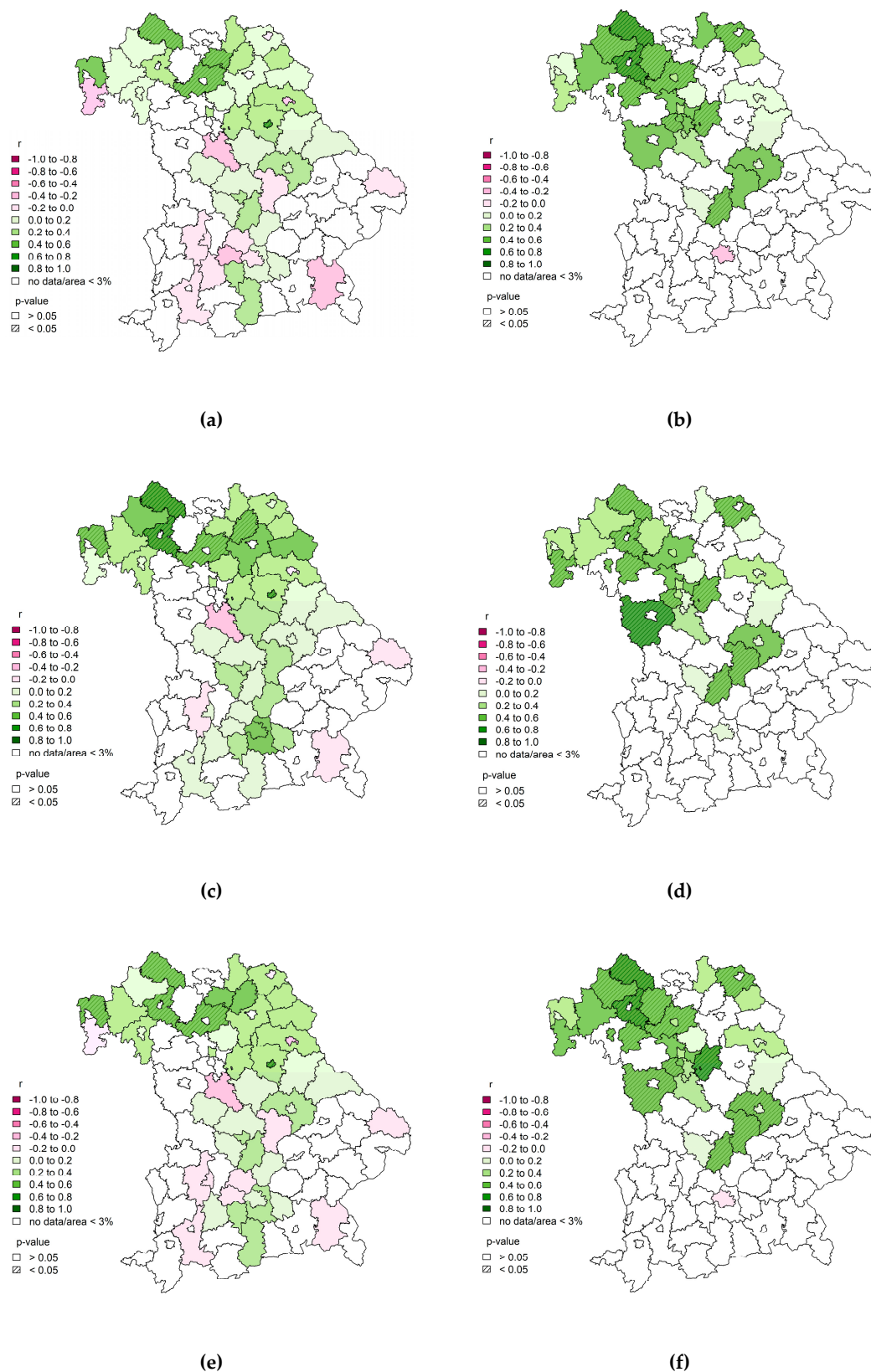


Figure S11. Bravais-Pearson correlation coefficients between the relative annual summer barley yield anomalies and the annual mean TCI (a)/VCI (c)/VHI (e) and the relative annual winter rye yield anomalies and the annual mean TCI (b)/VCI (d)/VHI (f) differentiated by county.

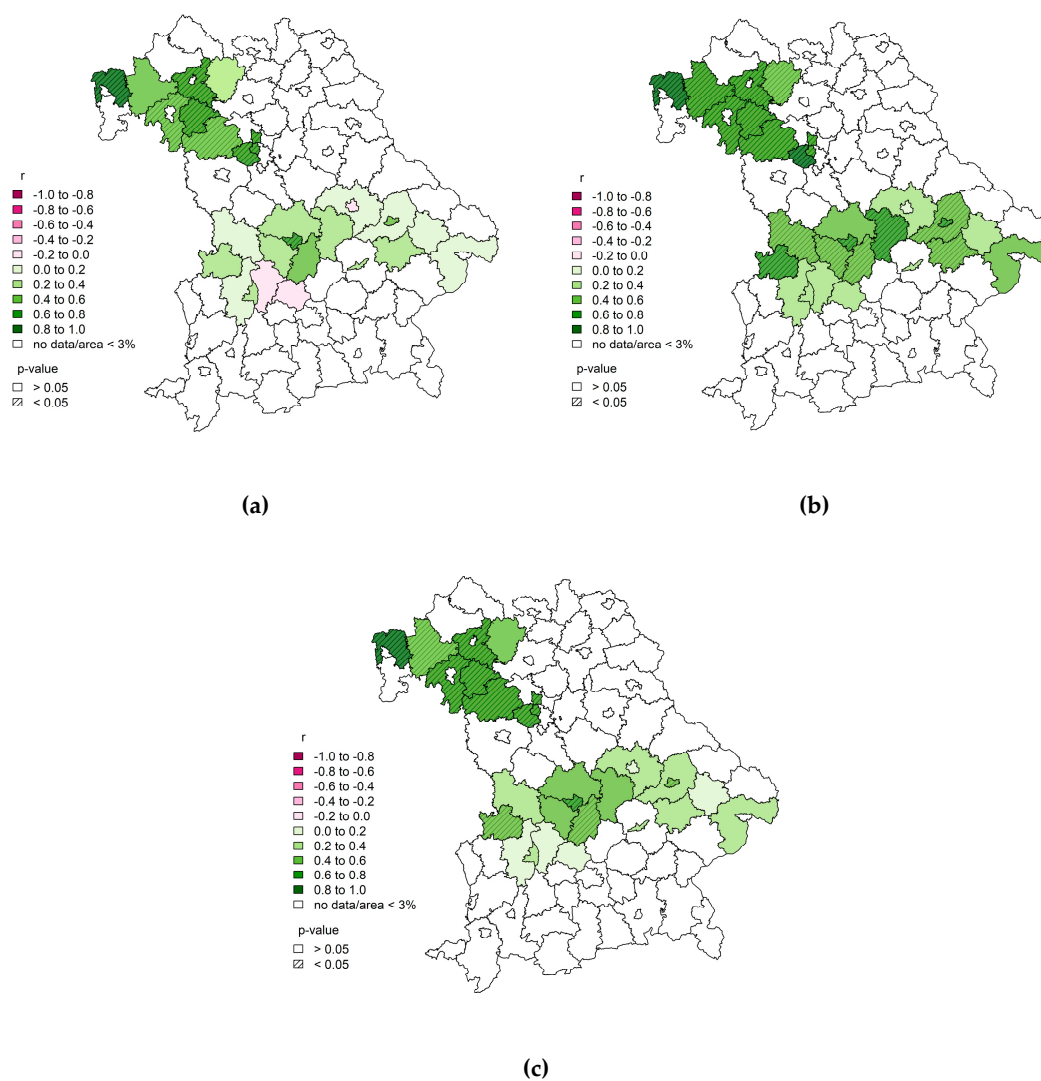


Figure S12. Bravais-Pearson correlation coefficients between the relative annual sugar beet yield anomalies and the annual mean TCI (a)/VCI (b)/VHI (c) differentiated by county.